International Journal of Engineering Research & Technology (IJERT)
ISSN: 2278-0181
Vol. 4 Issue 06, June-2015

# Compressed Sensingbasedfor SAR Sparse Signal Reconstruction using L1-Regularized Least Square Algorithm

Nabil Girgis, Ahmed Saleh Amein
Military Technical College (MTC)
Cairo, Egypt

Hazem Zakaria,M. Abo Elenean El Desoky
Military Technical College (MTC)
Cairo, Egypt

***Abstract*— Synthetic Aperture Radar (SAR) Imaging techniques now form an important field in remote sensing; the high-resolution images from aircraft and satellites are now used for terrain mapping and target identification, and many other applications. Targeting based missions which represented in the military surveillance and reconnaissance usually results in a very high dynamic range SAR images caused by a few very bright objects (manmade objects) and many low scattering coefficients (background).The proposed algorithm used the Compressive Sensing CS framework for exploiting this image data nature (represented in the redundancy in the data modeled as sparsity) in compressing SAR Images based on L1-regularized Least Square algorithm for reconstructing compressed data which enhance the overall system performance such as reduction of the onboard memory requirements and improvement of the downloadtransmission link capabilities for downloading the large amount of data produced by the high resolution SAR images.**

***Keywords—SAR image compression; Compressive Sensing***

## I.INTRODUCTION

Synthetic-Aperture Radar (SAR) has seen wide applications in remote sensing and mapping. Synthetic aperture radar technology has provided terrain structural information to geologists for mineral exploration, oil spill boundaries on water to environmentalists, sea state and ice hazard maps to navigators, and reconnaissance and targeting information to military operations.

Synthetic aperture radar (SAR) is a radar imaging technology that is capable of producing high-resolution images of the stationary surface targets and terrain.The high resolution in the range direction is achieved by using large bandwidth signals while the high resolution in the azimuth direction is achieved by synthesizing a large aperture using platform motion [2]. The SAR data collection geometry requires that the received data has to be focused before obtaining an image comprehensible to the human eye. The generated data had to be stored on-board or transmitted to a ground station via a dedicated data link. Therefore, some form of compression on the raw data provides an attractive option for SAR systems design. SAR systems in practice mostly use the simplest methods because of their low computational requirements; recently an attractive idea is to apply results of the rapidly developing field of compressed sensing in compressing SAR data. Unlike traditional compression/decompression methods, compressed sensing allows very simple non-adaptive compression schemes at the expense of a significantly increased complexity for the decompression [1], [5], [7].

The key idea is to exploit redundancy in the data modeled as sparsity in an appropriate dictionary. The novel theory of compressive sensing (CS) — also known under the terminology of compressed sensing, compressive sampling or sparse recovery.

In this paper we introduce a proposed compressive sensing (CS) compression scheme for compressing a high dynamic rang SAR images based on L1-Least Square algorithm for reconstructing compressed data. The quality of images produced by proposed algorithm is evaluated using image quality parameters measurements such as Mean Square Error (MSE), Peak Signal to Noise Ratio (PSNR) and Relative Error (RE). This Project is implemented in MATLAB and a few visualization enhancement features, which facilitates processing data and producing desired output.

## II.SAR IMAGE DATA NATURE AND BASIC PROPERTIES

### *A. SAR Image data nature*

SAR data is acquired from a moving platform by emitting at close intervals a band pass microwave radar signal in direction of a specific area, or scene as illustrated in Fig.1, and sampling the signal backscattered by the ground objects. When the size of the scene is small compared to its distance to the radar platform, the curvature of the wave front of the radar signal over the scene can be neglected. This approximation results in a simple interpretation of SAR data in the Fourier domain (2D Fourier transform of the scene) and is the basis of a SAR processing technique referred to as “polar format algorithm”. In this approximation, each received signal only contains information averaged over the scene in a direction orthogonal to the direction of propagation of the emitted radar signal [9].

In the Fourier domain, each received signal thus contains information included in a radial line orthogonal to the averaging direction, i.e. in the direction of propagation. Consequently, the whole SAR data approximately correspond to a polar grid in the Fourier domain, a natural consequence of this bandpass property is that SAR images are complex-valued. In order to form the SAR image, the polar grid data

are interpolated to a rectangular grid from which the image is computed by means of an inverse DFT.

In practice, the angular range of the polar grid is often very small, in which case the polar grid can already be well approximated by a rectangular grid. For this reason, we will simply assume in this paper that the raw data correspond to the 2D Fourier transform of the SAR image.

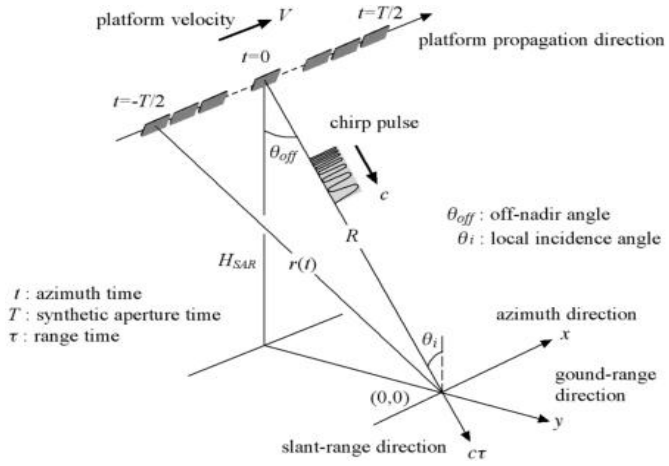


Fig.1. shows the SAR data acquisition system.

### *B. SAR Image properties*

There are three main properties of SAR images; the first one is the noise-like characteristics of SAR images. The second one is their often very high dynamic range caused by a few very bright objects and finally the compressibility of SAR Images.

- Noise-Like Characteristics:As the output of a coherent imaging system, SAR images are extremely noisy. This feature comprises two aspects. First, the magnitude of the SAR image contains what is referred to as speckle noise which can be efficiently modeled as multiplicative exponential white noise. Second, the phase of the image can also be modeled as uniform white noise in $[0,2\pi]$.
- Dynamic Range: In General, the radiation emitted by the radar antenna is scattered when hitting the ground and only a very small proportion of the energy is reflected in the direction of the antenna. This typically happens in natural areas without any man-made objects. However, in some cases, a much larger proportion of the energy is reflected towards the antenna. A well-known cause for this phenomenon is the presence of corner shapes which are very common in man-made objects, building or vehicles. As a consequence, SAR images containing man-made objects typically have very bright pixels located on those objects while the background of the image is much darker. Moreover, these bright pixels are usually highly localized. For a building, only a few edges and corners appear as very bright in the SAR image. In practice, the brightest pixels of a SAR image can typically be $(10^3)$ times larger than the background pixels.
- Compressibility of SAR images:Due to their noise-like properties, complex-valued SAR images are very difficult to compress efficiently, unlike images without noise that have the same good compression properties as in most natural images. However the multiplicative noise provides the whole image with high entropy, thus significantly reducing its compressibility in any dictionary. For this reason, typical sparsifying transforms used in image processing such as wavelet transforms do not result in good sparse approximations for SAR images.

## III. COMPRESSED SENSING BASED ACQUISITION FOR SAR

According to compressed sensing theory, a discrete signal or image expressed as a vector $f \in \mathrm{R}^{\mathrm{N}}$can be exactly reconstructed with a reduced number of samples compared to the Nyquist rate provided that it is sparse in some basis: $f=\Psi x$where $\Psi \in \mathrm{R}^{\mathrm{N}\times\mathrm{N}}$ is a matrix whose columns are the basis vectors, and$x \in \mathrm{R}^{\mathrm{N}}$ is a vector with a small number of non-zero components K<< N [14].

In a compressed sensing framework [9], the signal/image is acquired through linear projections: $y = \Phi f$, where $y \in \mathrm{R}^{\mathrm{M}}$is the measurement vector and $\Phi \in \mathrm{R}^{\mathrm{M}\times\mathrm{N}}$is referred to as the measurement matrix, considering the *k*-sparse representation *x* which results in the measurement equation.

$$y = \Phi\Psi x. \qquad (1)$$

In order to recover a *k*-sparse vector *x*, the number of measurements M must be at least greater than *k* but can be significantly smaller than the signal/image dimension K<M<<N. While this cannot be achieved with any combination of measurement matrix and basis, it has been shown that several classes of random measurement matrices allow it for any basis with high probability.Given the measurements y, the reconstruction of the sparse vector *x* can beachieved by searching for the sparsest vector $\tilde{x}$ compatible with the measurements [11].

This is usually referred to as the $\ell_0$ optimization problem where $x = \mathrm{argmin}_{\tilde{x}}\|\tilde{x}\|_0$ subject toy $= \Phi\Psi\tilde{x}$, where the pseudo-norm$\|\,.\,\|_0$corresponds to the number of non-zero elements. As it is well known, this is a combinational problem which cannot be solved directly in practice. The two most common approaches are therefore to replace it with an $\ell_p$optimization problem with$0< p \leq 1$or to use a greedy algorithm such as Orthogonal Matching Pursuit.

In order to define a compressed sensing based acquisition scheme for SAR images, three elements must be specified: a basis where the data are assumed sparse (or close to sparse), a measurement operator and a reconstruction algorithm, these aspects shall be discussed below.

### *A. Sparse representation of SAR Images*

According to the statistics properties of SAR images which indicate that there is no basis or dictionary where the data can be assumed sparse. For this reason, it seems a priori impossible to acquire with a decent quality a whole SAR image in a compressed sensing framework. But, the very bright objects often related to man-made structures or vehicles are typically sparse in the space domain and slightly sparser in a wavelet domain. The image $f \in \mathrm{R}^{\mathrm{N}}$ can thus be decomposed into two components $f = f_s + f_n$, where $f_s$ corresponds to the sparse bright objects and $\mathrm{f_n}$ to the remaining non-sparse areas.

In this decomposition, the sparse component $f_s$ is typically larger than the other component because the bright objects are often several orders of magnitude brighter than the background of the image, thus compensating for their limited spatial support. If the image is represented in an orthonormal wavelet basis $\Psi$ this property is preserved, leading to a decomposition
$f = \Psi x_s + \Psi x_n$ where $x_s$ is sparse and larger than $x_n$. Thus, when bright objects are present, the whole SAR image can be assumed close to sparse in a wavelet basis.

Fig.2. shows an example of SAR images data sparsity property. This is because the bright objects in each SAR image often related to man-made structures or vehicles are typically sparse in the space domain, the number of resolution cells of bright objects man-made objects (useful targets) in the received SAR image is typically much smaller than the number of resolution cells of natural areas without any man-made objects (background scattering coefficients) in the illuminated scene by the SAR system [10].

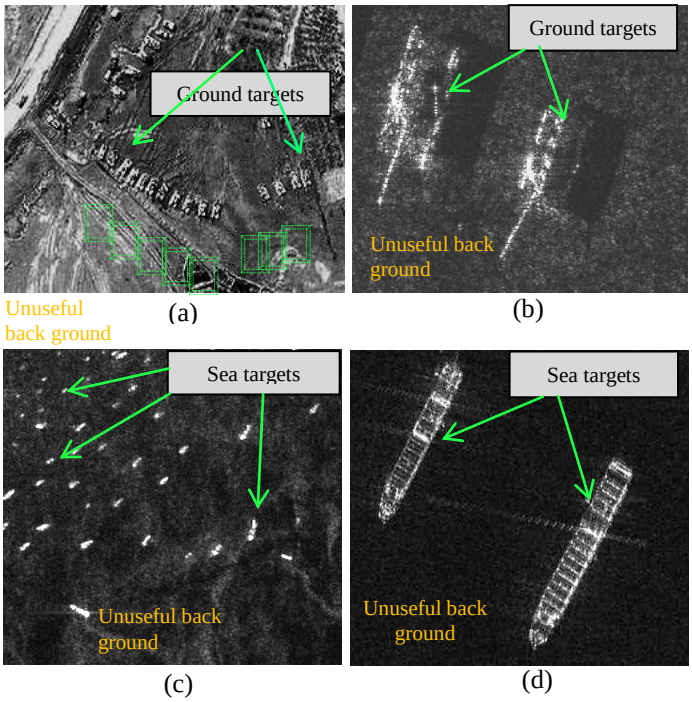


Fig.2. Examples of SAR images data sparsity property.

Fig.2. (a), (b) Shows SAR images of a ground forces, many ground targets (tanks) can be seen as bright spots in this images due to corner reflections with low background scattering coefficients .in (c), (d) Shows another SAR images of an area of the sea near a busy port, many sea targets (ships) can be seen as bright spots in this images due to corner reflections.

### *B. Designing Sensing Matrix (Measurement Operator)*

As previously mentioned, SAR raw data can be assimilated to samples of the Fourier transform of the SAR image. Among the classes of generic measurement matrices used for compressed sensing, this naturally calls for the partial Fourier matrix [4], [6], [8] class where the measurements y correspond to uniformly randomly selected Fourier coefficients of the SAR image. If $F \in R^{N\times N}$ is the matrix representing the 2D DFT operator, we define the measurement matrix $\Phi^{M\times N}$ as a random subset of M lines of F.

The incoherence property of the matrix, $\Phi$, is used to ensure that the matrix, $\Phi$, is sparse matrix by determining the number of measurements, M, by:

$$M \geq \text{const } k \log\frac{N}{k}$$

Where, M, is the number of measurements, N, is the number of Nyquist rate samples (length of the SAR image data), k, is the number of the highest scattering coefficients, and (Const) is considered as the under sampling factor, its value is determined according to desired reduction ratio in the SAR image data length.

### *C. Reconstruction algorithms*

There are different types of algorithms which are used for sparse reconstruction such as convex optimization algorithms which require very few measurements but are computationally more complex. On the other extreme are combinatorial algorithms, which are very fast, but require many measurements that are sometimes difficult to obtain. Greedy algorithms are in some sense a good compromise between those extremes concerning computational complexity and the required number of measurements; in this paper we introduce one of the most powerful convex optimization algorithm in sparse reconstruction of SAR data which so called L1-regularized Least Square algorithm.We will illustrate this method on a simulated and real SAR imaging data in the next section IV.

## IV. L1- REGULARIZED LEAST SQUARE ALGORITHM

We consider a linear model of the form

$$y = Ax + v,$$

Where $x \in R^n$ is the vector of unknowns (original signal/Image), $y \in R^m$ is the vector of observations, $v \in R^m$ is the noise, and $A \in R^{m\times n}$ is the data matrix [12].

When $m \geq n$ and the columns of $A$ are linearly independent, we can determine $x$ by solving the least square problem of minimizing the quadratic loss $\|Ax - y\|_2^2$, where $\|x\|_2 = (\sum_i x_i^2)^{1/2}$ denotes the $\ell_2$-norm of $x$.

When $m$, the number of observations, is not large enough compared to $n$, simple least-squares reversion leads to over-fit, so a standard technique to prevent over-fitting is $\ell_2$-regularization [ ], which can be written as

$$minimize\ \|Ax - y\|_2^2 + \lambda\|x\|_2^2 \quad (2)$$

Where $\lambda > 0$ is the regularization parameter.

$\ell_1$-Regularized Least Squares. Substitute a sum of absolute values for the sum of squares used in $\ell_2$-regularization (2), to obtain

$$minimize\ \|Ax - y\|_2^2 + \lambda\|x\|_1 \quad (3)$$

Where $\|x\|_1 = \sum_i^n |x_i|$ denotes the $\ell_1$ norm of x and $\lambda > 0$ is the regularization parameter, equation (3) stand for $\ell_1$-regularized LSP. This problem always has a solution, but it need not be unique. We list some basic properties of $\ell_1$-regularized LS, shows the differences with the $\ell_2$-regularized LS.

- *Nonlinearity*. From (2) shows the $\ell_2$-regularization produces a vector *x, which* is a linear function of the observation vector *y.* by contrast $\ell_1$-regularized LS, which is not linear in *y*.
- *Limiting behavior as* $\lambda \to 0$. Unlike $\ell_2$-regularized LS as $\lambda \to 0$. $\ell_1$-regularized LS, the limiting point has the minimum $\ell_1$-norm among all points that satisfy $A^T(Ax - y) = 0$.
- *Finite convergence to zero as* $\lambda \to \infty$. For $\ell_2$-regularized LS, the optimal solution tends to zero, as $\lambda \to \infty$. For $\ell_1$-regularized LS, however the convergence occurs for a finite value of λ:

$$\lambda \geq \lambda_{max} = \|2A^T y\|_\infty \qquad (4)$$

Where $\|x\|_\infty = max_i |x_i|$ denotes the $\ell_\infty$-norm of the vector *x*. For $\lambda \geq \lambda_{max}$, the optimal solution of the $\ell_1$-regularized LSP (3) is 0. In contrast, the optimal solution to the $\ell_2$-regularized LSP is zero only in the limit *as* $\lambda \to \infty$.

Recently, the idea of $\ell_1$-regularization has been receiving alot of interest in signal processing and statistics. In signal processing, the idea of $\ell_1$-regularization comes up in several contexts including basis pursuit denoising [13] and a signal recovery method from incomplete measurements. Some of these problems do not have the standard form (3) but have a more general form

$$minimize \ \|Ax - y\|_2^2 + \sum_{i=1}^n \lambda_i |x_i| \qquad (5)$$

Where $\lambda_i \geq 0$ are regularization parameters (The variables $x_i$ that correspond to $\lambda_i = 0$ are not regularized). This general problem can be reformulated as a problem of the form (3).

## V. Proposed Algorithm Ofsar Sparse Signal Reconstruction Using $L_1$-Regularized LS

Let Z be an unknown vector in $R^n$. Suppose that we have *m* linear measurements of an unknown signal/image $Z \in R^n$

$$y_i = \langle \phi_i, Z \rangle + \nu_i, \qquad i = 1, \dots, m$$

Where $\langle \cdot, \cdot \rangle$ denotes the usual inner product, $\nu \in R^m$ is the noise, and $\phi_i \in R^n$ are known signals. Traditional reconstruction methods require at least n samples. Suppose we know a prior knowledge that Z is compressible or has a sparse representation in a transform domain, descried by $W \in R^{n \times n}$ (after expanding the real and imaginary parts of the SAR image coefficients). In this case, if $\phi_i$ are well chosen, then the number of measurements m is intensely smaller than the size n which is necessary [13].

Compressed sensing or compressive sampling [11] attempts to exploit the sparsity or compressibility of the true (signal/SAR image) in the transform domain by solving a problem of the form

$$minimize \ \|\Phi Z - y\|_2^2 + \lambda \|WZ\|_1 \qquad (6)$$

Where the variable is $Z \in R^n$, $\Phi = [\phi_1, \dots, \phi_m]^T \in R^{m \times n}$ is called the compressed sensing matrix, $\lambda > 0$ is the regularization parameter, and Wis called the sparsifying transform.

When *W*is invertible, we can reformulate the compressed sensing problem (6) as the $\ell_1$-regularized LSP

$$minimize \ \|Ax - y\|_2^2 + \lambda \|x\|_1 \qquad (7)$$

Where the variable is $x \in R^n$ and the measurement matrix $A = \Phi W^{-1} \in R^{m \times n}$ and $y \in R^m$.

We will illustrate this method on a simulated and real SAR imaging data set.After the SAR images is passes through the image formation process steps it goes through the compression module for storing and or download to the ground station. The reconstruction algorithm based on $\ell_1$-regularized LS is used for reconstructing the original signal/Image data.

In order to assess the performance of the proposed method many measuresof image quality such as (MSE, NMSE, PSNR and RE) is performed for performance evaluation of the proposed algorithm [8].

- *Mean Square Error MSE.*The mean square error is one of the most commonly used performance measures in image and signal processing. For an image of size N × M it can be defined as follow,

$$MSE = \frac{1}{NM} \sum_{n=0}^{N-1} \sum_{m=0}^{M-1} |x[n,m] - \hat{x}[n,m]|^2$$

Where x[n, m]the original image and x̂[n, m] is the decompressed image.

- *Normalized Mean Square Error MSE.* MSE is normalized with the variance of the original signal to give NMSE,

$$\boldsymbol{NMSE = \frac{\sum_{n=0}^{N-1} \sum_{m=0}^{M-1} |x[n,m] - \hat{x}[n,m]|^2}{\sum_{n=0}^{N-1} \sum_{m=0}^{M-1} |x[n,m]|^2}}$$

- *Signal to Noise Ratio SNR.* SNR can be defined as,

$$\boldsymbol{SNR = 10\, log_{10} \frac{1}{NMSE}}$$

- *Peak Signal to Noise Ratio PSNR*. PSNR is the most commonly used performance measure for image processing applications. It can be defined as,

$$PSNR = 10\ log_{10} \frac{peak\ to\ peak\ value\ \ (original\ image)^2}{MSE}$$

- *Relative Error RE*. RE of reconstruction image is defined as follow,

$$RE = \left\{ \frac{\sum_{x=1}^{M} \sum_{y=1}^{N} [\mathrm{I}(x,y) - \hat{\mathrm{I}}(x,y)]^2}{\sum_{x=1}^{M} \sum_{y=1}^{N} [\mathrm{I}(x,y)]^2} \right\}^{1/2}$$

Where $\mathbf{I}(\boldsymbol{x},\boldsymbol{y})$ denotes the original image of scattering coefficients for illuminated scene, and $\hat{\mathbf{I}}(\boldsymbol{x},\boldsymbol{y})$ is the reconstructed one. Apparently, the lower the value of RE is, the better the reconstructed performance will be.

## VI. Simulation and Results

In order to assess the performance of the proposed algorithms using the compressive sensing framework, we consider two case studies (Fig. 3, Fig 5). First case ; Simulated SAR image of bouing 727 airplane with very bright objects, second case; two real SAR images of sea targets at two different territories from two different sensors. Typical results of the proposed method are shown in (Fig.5).

### *A. Case 1: Simulated SAR Image*

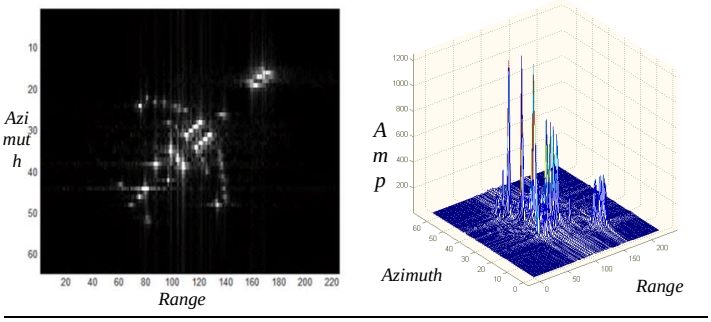


Fig.3 Simulated SAR Image with the 3-D Magnitude plot.

Fig.3 shows a simulated SAR image of bouing 727 aircraft at the left side with data files are written as a complex 2-D matrix, at the right side the 3-D amplitude plot describe the data value of each cell. Each row of the matrix corresponds to a range cell, and each column corresponds to a pulse in a burst,for each pulse, 64 complex range samples were saved. The file contains 256 successive pulses. Motion compensation and range processing have been applied to the data.The proposed algorithm is checked for the simulated image using different subsampling ratios (missing samples).

Fig.4 shows examples of test image after reconstructionusing the proposed method at different subsampling ratios,

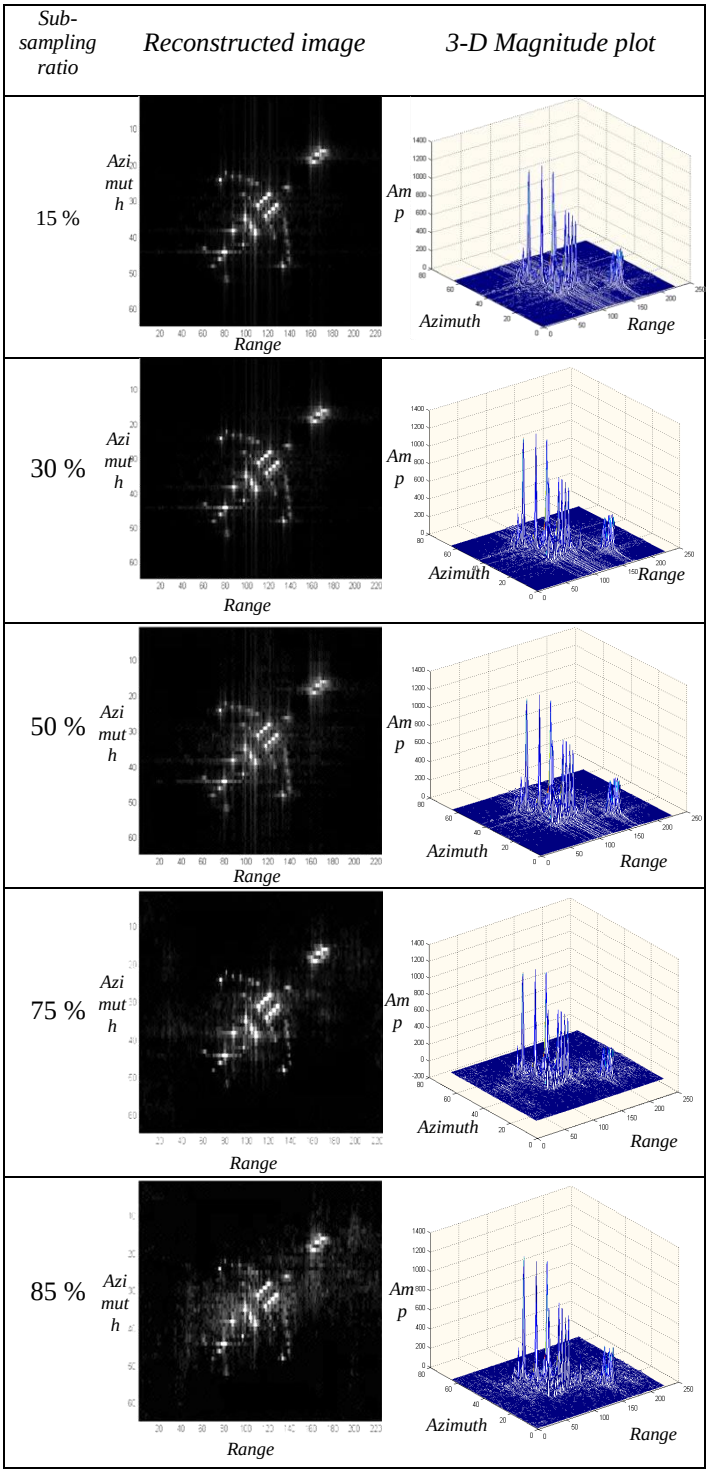


Fig.4. Example of the simulated Image after the reconstruction with the proposed algorithm at different sub-sampling ratios.

The first column corresponds to the subsampling ratio (Compression Ratio), the second column corresponds to the reconstructed images, and the last column corresponds to the 3-D amplitude plot of the reconstructed image.

Table.1. shows the Mean Square Error MSE, Peak Signal to Noise Ratio PSNR and the Relative Error RE respectively

between the original and the reconstructed images using the proposed methods for different subsampling ratio.

| Sub-sampling ratio | Mean square error (MSE) | Peak signal to noise ratio (PSNR)/ dB | Relative error RE |
|---|---|---|---|
| 15 % | 0.0885 | 72.483 | 0.0066 |
| 30 % | 0.7783 | 63.041 | 0.0197 |
| 40 % | 1.777 | 59.455 | 0.0297 |
| 50 % | 4.296 | 55.621 | 0.0462 |
| 60 % | 10.938 | 51.563 | 0.0737 |
| 75 % | 62.904 | 43.966 | 0.1767 |
| 85 % | 124.17 | 41.012 | 0.2482 |

Table.1. MSE, PSNR and RE of the test image at different sub-sampling ratios.

The values show that as the subsampling ratio (compression ratio) increases the (MSE) and relative error (RE) increases on the other hand the (PSNR)decreases and vise-versa.

Here the proposed method gives a perfect performance in reconstructing the original signal/image in case of lower subsampling (Between 15 % and 50 % missing samples), and an acceptable performance in case of moderate subsampling (Between 50 % and 75 % missing samples), and a poor quality in recovery of the original signal/image in case of higher subsampling (More than 75 % missing samples).

*B. Case 2: Real SAR Images*

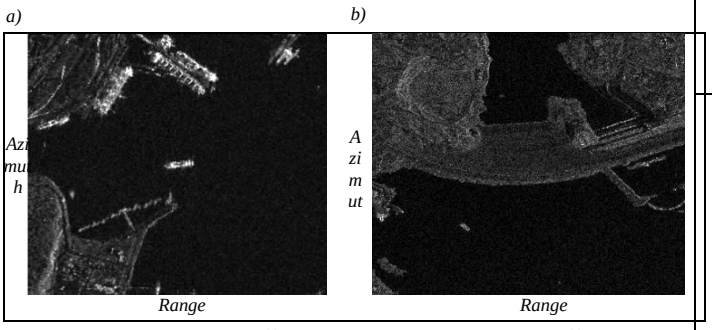


Fig.5.Real SAR Images in different locations acquired by two different sensors.

Fig.5.a),b) shows real SAR images of sea targets (ships), which looks like very bright spots due to corner reflections with low background scattering coefficient describing the flat areas sea/ground. In order to make it simpler we take subset images (256 × 256) pixels as in (fig.6) to use it with the proposed method of compressing and reconstructing the original image data with lower computational time.

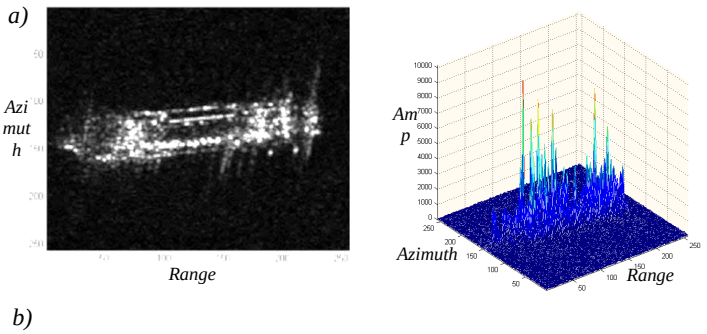


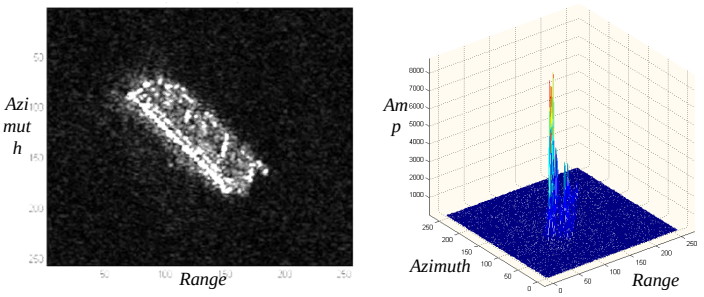


Fig.6. Real SAR Images of two different sea targets.

Fig.6.a),b)shows a subset SAR imagesfrom (fig.5) of two different Sea targetswith size (256 x 256) at the left side andwith data files are written as a complex 2-D matrix, at the right side the 3-D amplitude plot describe the absolute data value of each cell.

Next (fig.7) are examples of real SAR imagesafter reconstructionusing the proposed method at different subsampling ratio (missing samples).

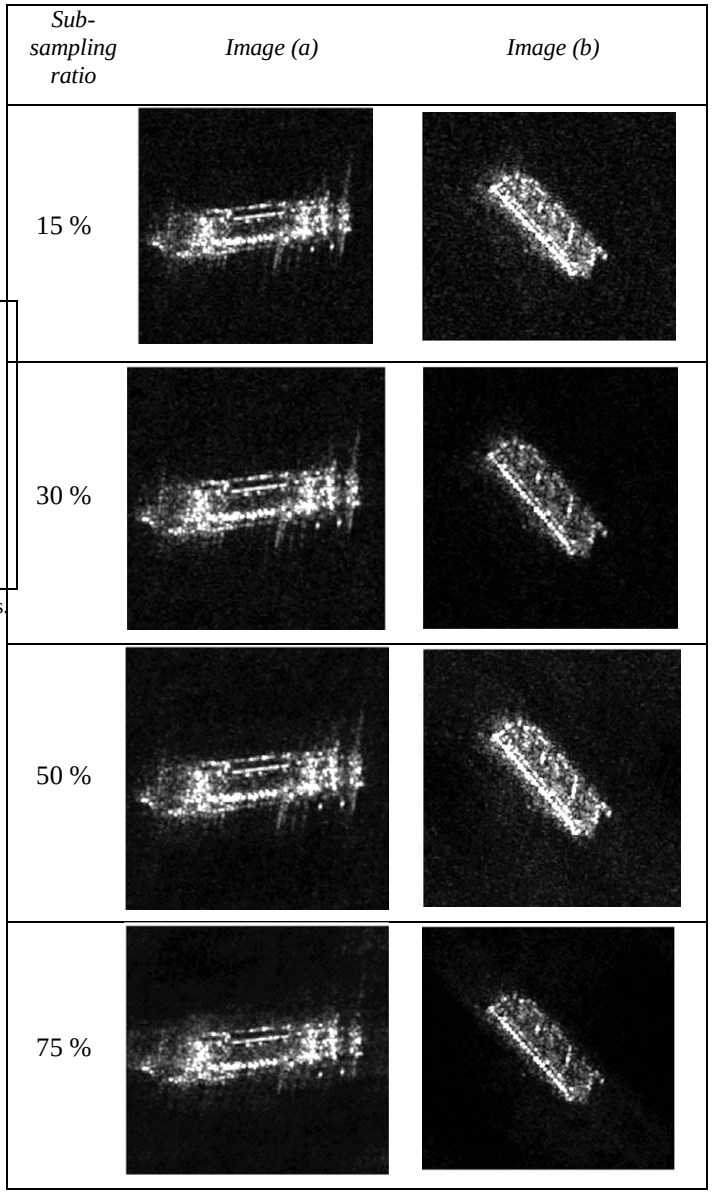

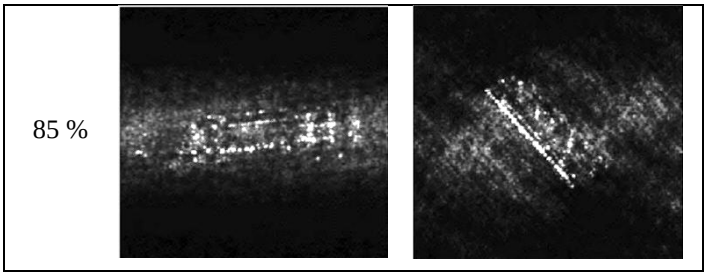


Fig.7. Real SAR Images after reconstruction with the proposed method.

The first column corresponds to the subsampling ratio (Compression Ratio), the second column corresponds to the reconstruction of image (a), and the last column corresponds to the reconstruction of image (b).

In case of lower subsampling (Between15 % and30 % missing samples), we observe that the$\ell_1$-regularized LS allows a perfect recovery of the main objects (targets), as well as the flat background area has the same performance of recovering the original signal.

In case of moderate subsampling (Between50 % and75 % missing samples), we observe that the $\ell_1$-regularized LS allows the recovery of the main objects (targets), However the flat areas where the statistics of the images are similar to stationary white noise are almost recovered with little distortion.

In case of higher subsampling (More than 75 % missing samples), we observe that the $\ell_1$-regularized LS allows an approximated recovery of the main objects (targets) with lower quality, and an apparent distortion in the flat background areas.

Table.2. shows the Mean Square Error MSE, Peak Signal to Noise Ratio PSNR and the Relative Error RE respectively between the original and the reconstructed images using the proposed methods for different subsampling ratio, using the real SAR images.

| Sub-sampling ratio | (MSE) | | (PSNR) / dB | | Relative error RE | |
|---|---|---|---|---|---|---|
| | *Image (a)* | Image (b) | Image (a) | Image (b) | Image (a) | Image (b) |
| 15 % | 105.252 | 68.797 | 59.9002 | 60.5307 | 0.0276 | 0.0319 |
| 30 % | 238.39 | 137.461 | 56.3496 | 57.5246 | 0.0416 | 0.045 |
| 40 % | 347.209 | 183.009 | 54.7166 | 56.2817 | 0.0502 | 0.0519 |
| 50 % | 572.427 | 256.738 | 52.5453 | 54.8115 | 0.0645 | 0.0615 |
| 60 % | 956.89 | 342.897 | 50.3139 | 53.5548 | 0.0833 | 0.0711 |
| 75 % | 2675 | 742.103 | 45.8492 | 50.2018 | 0.1393 | 0.1046 |
| 85 % | 17725 | 7357.5 | 37.636 | 40.239 | 0.3587 | 0.3294 |

Table.2. MSE, PSNR and RE of the real images at different sub-sampling ratios.

Table.2. shows that by increasing the subsampling ratio (compression ratio) results inincreasing the (MSE) and relative error (RE) on the other hand the (PSNR)decreases.

By analyzing these results (fig.8) shows the graph of the NMSE analysis curve and (fig.9) shows the graph of the PSNR analysis.

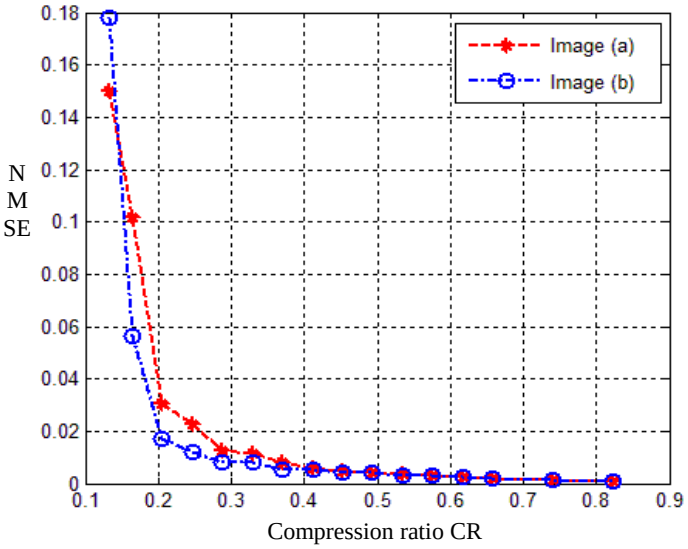


Fig.8. Graph for NMSE analysis at different compression ratios.

From the Fig.8, it can be seen that as the compression ratio increases over (CR> 0.3 0r missing samples < 70 %) the Normalized Mean Square Error NMSE decreases, which means that the images are perfectly recovered with very high quality, and for the lower compression ratio ( CR< 0.3 or missing samples > 70 % ) the NMSE increases, which means that the images are poorly recovered with low quality, the apparent changes in NMSE at lower CR between image (a) and image (b) is due to the variation of the dynamic range of each image

Also the Peak Signal to Noise Ratio PSNR graph (Fig.9) can used in evaluating the proposed algorithm, by get a relation between compression ratio and the value of the PSNR, it can be seen that, as the compression ratio increases over (CR > 0.3 0r missing samples < 70 %) the value of the PSNR is greater than (45 dB) which considered the recovered image as an excellent image.

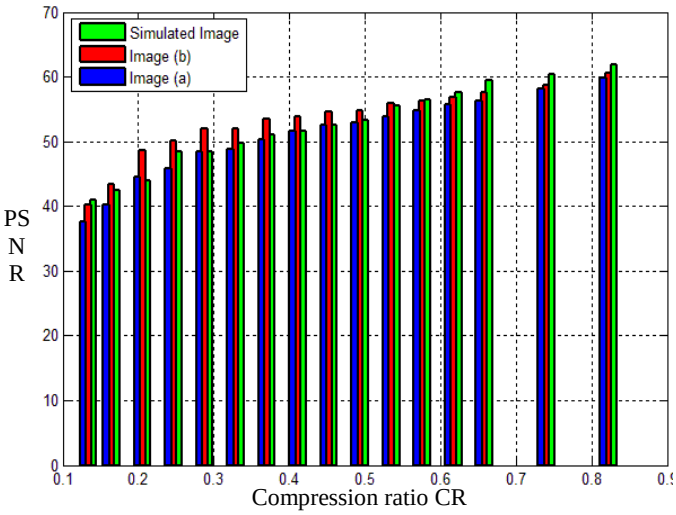


Fig.9. Graph for PSNR analysis at different compression ratios.

## VII. CONCLUSION

This paper presents a sparse reconstruction method for SAR imaging based on CS theory, which aims to sparse targets reconstruction using less samples than Nyquist samples by solving $\ell_1$-regularized Least Square problem LSP.

The presented method greatly improves the imaging performance of SAR, when the target space is sparsein a very high dynamic range SAR images caused by a few very bright objects (manmade objects) and many low scattering coefficients (background). Simulated results show a superior performance of the presented method which significantly suppresses the distortions of the main objects (targets) at higher subsampling ratios.This can enhance the overall system performance such as reduction of the onboard memory requirements and improvement of the download transmission link capabilities for downloading the large amount of data produced by the high resolution SAR images.

## REFERENCES

[1]D. Donoho, "Compressed sensing," IEEE Trans. Inf. Theory , vol.52,no. 4, pp. 1289–1306, Apr. 2006.

[2]D. Donoho and Y. Tsaig,"Fast solution of l1 -norm minimization prob-lems when the solution may be sparse," Manuscript 2006 [Online].Available: http://www.stanford.edu/

[3]D. Donoho, M. Elad, and V. Temlyakov, "Stable recovery of sparseOvercomplete representations in the presence of noise," IEEE Trans.Inf. Theory , vol. 52, no. 1, pp. 6 –18, Jan. 2006.

[4] E.J.Cand`es, J.Romberg, and T.Tao, "Robust uncertainty principles:Exact signal reconstruction from highly incomplete frequency information," IEEE Trans. Info. Theory, vol. 52, no. 2, pp. 489–509, Feb. 2006.

[5]Compressive sampling Emamnuel J. Candès Proceedings of the International Congress of Mathematicians, Madrid,Spain,2006

[6] Development of Compression Algorithms for Remotely Sensed SAR Data (IJESIT) Volume 2, Issue 4, July 2013.

[7]Sparse Reconstructionfor SAR imagingbased on CS.S.-J. Wei, X.-L. Zhang, J. Shi, and G. Xiang,Chengdu 610054, China.

[8]SyntheticApertureRadar(SAR)ImageCompression.GunerArslanandMages hValliappan

[9] Compressed sensing based compression of SAR raw data.Gabriel Rilling, Mike Davies and Bernard Mulgrew.University of Edinburgh.United Kingdom.

[10]E. Candès, J. Romberg, and T. Tao, "Stable signal recovery from in-complete and inaccurate measurements," Commun. Pure Appl. Math.,vol. 59, no. 8, pp. 1207–1223, 2005.

[11]J. Fuchs, "Recovery of exact sparse representations in the presence ofnoise," IEEE Trans. Inf. Theory , vol. 51, no. 10, pp. 3601 –3608, Oct.2005.

[12] E. Hale, W. Yin, and Y. Zhang, "A fixed-point continuation method for l1-regularized minimization with applications to compressed sensing, "Manuscript 2007 [Online]. Available: http://www.dsp.ece.rice.edu/cs/

[13]An Interior-Point Method for Large-Scale L1-Regularized Least SquaresSeung-Jean Kim , Member, IEEE , K. Koh, M. Lustig, Stephen Boyd , Fellow, IEEE, andDimitryGorinevsky, 2007.

[14]Matthew Herman and Thomas Strohmer. Compressed sensing radar.Acoustics, Speech and Signal Processing, 2008. ICASSP 2008. IEEEInternational Conference on, pages 1509–1512, 31 2008-April 4 2008.